ELSEVIER

Journal of Contaminant Hydrology 24 (1996) 53–73

JOURNAL OF
Contaminant
Hydrology

Transport of rate-limited sorbing solutes in an aggregated porous medium: A multiprocess non-ideality approach

Qinhong Hu [a,*], Mark L. Brusseau [a,b]

[a] *Department of Soil, Water and Environmental Science, University of Arizona, Tucson, AZ 85721, USA*
[b] *Department of Hydrology and Water Resources, University of Arizona, Tucson, AZ 85721, USA*

Received 14 July 1995; accepted 21 February 1996

Abstract

The purpose of this work is to investigate the transport of rate-limited sorbing solutes in a saturated, aggregated porous medium. Data obtained from miscible displacement experiments are used to examine the transport of solutes constrained by rate-limited sorption and mass transfer, to examine the synergistic effects of two non-ideality factors, and to test the capability of a multiprocess non-equilibrium (MPNE) model to simulate transport. The input parameters were obtained independently, allowing the model to be used in a predictive mode. The independent predictions obtained with the MPNE model provided very good descriptions of the experimental data for several organic solutes with different structures. The effects of multiple non-ideality factors controlling solute transport were explored, and flow interruption experiments provided additional evidence regarding the synergistic effects of rate-limited sorption and rate-limited mass transfer. Our analyses have shown quantitatively that both mass distribution and characteristic reaction time are important factors influencing transport. Solute characteristics controlled the degree to which each factor influenced transport behavior for a given porous medium. The velocity dependency of the mass-transfer and desorption rate coefficients and the resultant impact on solute transport were also examined.

Keywords: transport; mass transfer; rate-limited sorption

1. Introduction

Transport of reactive solutes can be influenced by a number of factors that can cause non-ideal behavior [see Brusseau (1994) for a review], which is transport that does not

* Corresponding author.

PII S0169-7722(96)00006-X

coincide with that predicted with models based on assumptions of porous medium homogeneity and instantaneous mass transfer. For example, solute transport in structured media often exhibits the effects of preferential flow and rate-limited diffusional mass transfer between advective and non-advective domains. Rate-limited sorption/desorption can also cause non-ideal transport. It is possible, under many situations, that more than one factor may contribute to non-ideal solute transport. For example, non-ideal transport of solutes caused by both physical non-ideality and rate-limited sorption has been reported by several authors (Kay and Elrick, 1967; Green et al., 1968; Davidson and McDougal, 1973; Rao et al., 1974; van Genuchten et al., 1977; Brusseau et al., 1989; Brusseau, 1991; Zurmuhl et al., 1991; O'Dell et al., 1992; Brusseau and Zachara, 1993; Veeh et al., 1994; Gaber et al., 1995). Accurate analyses of solute transport under these conditions can be accomplished only if all significant factors are considered. However, few previous analyses have explicitly considered multifactor, non-ideal solute transport. Moreover, the synergistic effects of multiple non-ideality factors have rarely been addressed.

The purpose of this research is to investigate the transport of rate-limited sorbing solutes in saturated, aggregated media and to examine the synergistic effects of two non-ideality factors. Data obtained from miscible displacement experiments will be used to examine the capability of a multi-process non-equilibrium (MPNE) model to predict the transport of solutes constrained by rate-limited sorption and rate-limited mass transfer. The input parameters will be obtained separately, allowing the model to be used in a predictive mode.

2. Materials and methods

2.1. Materials

The following analytical-grade chemicals (Aldrich Chemical Co.) were used in the experiments: pentafluorobenzoate (PFBA), 2,4-dichlorophenoxyacetic acid (2,4-D), trichloroethene (TCE), chlorobenzene (cBENZ), and atrazine (from Supelco Inc.). $^{3}H_2O$ and ^{14}C-labeled 2,4-D were purchased from New England Nuclear and Sigma Chemical Co., respectively.

A soil, synthetic porous spheres, and silica-glass beads were used for the experiments. The soil was a sandy loam (sand: 77.7%, silt: 18.1%, clay: 4.2%, organic carbon: 1.36%, pH: 7.9 as determined by 1:1 soil/water extraction) and will be referred to as the Mixture soil (Estrella et al., 1993). The soil was sieved through 2-mm mesh prior to use. The synthetic porous spheres, with radii of 0.55 cm, have an average porosity 0.36 $cm^3\ cm^{-3}$. Details of the technique used to prepare the water-stable spheres from kaolinite clay suspension were described by Rao et al. (1980a). Silica-glass beads (212–300-μm diameter, Sigma Chemical Co.) were acid-washed before use.

2.2. Experimental procedures

2.2.1. System with rate-limited sorption

A preparative chromatography column made of precision-bore stainless steel (2.1-cm i.d., and 7.0-cm length; Alltech Associates Inc.) was used in the experiments employing

homogeneously packed Mixture soil. The column was incrementally packed with air-dry soil to obtain uniform bulk density. The packed column was slowly wetted from the bottom to establish saturation and ~ 50 pore volumes of electrolyte solution (5 m*M* $CaCl_2$) were pumped through the column prior to its use. This system was used to examine the sorption behavior of organic compounds in the Mixture soil. Values for sorption-related parameters will be obtained from this system.

2.2.2. System with physical non-ideality

The synthetic porous spheres were saturated with electrolyte solution for several days and were packed into a Plexiglas column (7.6-cm i.d., 15.0-cm length) along with glass beads. The column was packed in incremental steps in the presence of the electrolyte solution to establish uniform bulk density. This medium consisted of a distinct bimodal pore-size distribution, comprised of microporosity within the porous spheres and macroporosity between the spheres. The system was used to examine sorptive and diffusive interactions of solutes with the porous spheres and to evaluate the applicability of the dual-porosity solute transport model based on first-order mass transfer between advective–nonadvective domains.

A separate column packed with solid glass spheres (0.5-cm radius) and glass beads was used to derive dispersive characteristics of the system. The ratio of solid-spheres volume to the column volume was the same as that for the corresponding column with porous spheres.

2.2.3. System with both physical and sorption non-ideality

Porous spheres identical to those described above were packed, in a similar manner, with Mixture soil to investigate the transport of rate-limited sorbing solutes in a sorptive, aggregated medium. By doing so, a system with both physical non-ideality and rate-limited sorption was developed. The well-defined system was employed to allow derivation of independently determined parameter values, which will be used to attempt to predict the experimental results. Preliminary results showed that sorption of tested organic compounds by the Plexiglas column apparatus (packed with glass beads only) was negligible compared to the sorption of the organic compounds by the Mixture soil.

2.3. Miscible displacement

The apparatus and methods employed for the miscible displacement studies were similar to those used previously (Hu and Brusseau, 1995). One single-piston HPLC pump (SSI Model 300 or Gilson Model 305) was connected to the column, with a three-way switching valve placed in-line to facilitate switching between solutions with and without the solute of interest. A flow-through, variable-wavelength UV detector (Gilson, Model 115) was used to continuously monitor concentrations of solutes in the column effluent. Output was recorded on a strip-chart recorder (Fisher, Recordall Series 5000). For experiments with the slow pore-water velocity and for those in which radio-labelled compounds were used, effluent fractions were collected with an automated fraction collector (Pharmacia RediFrac). Concentrations of PFBA, *2,4*-D, and atrazine were determined by analysis with a UV–VIS spectrophotometer (Hitachi Model

U2000). The activities of radio-labelled compounds in the effluent samples were analyzed by radioassay using liquid scintillation counting (Packard Tri-Carb Liquid Scintillation Analyzer, Model 1600TR).

The initial concentrations of solutes used in the experiments were 100 mg l^{-1} (PFBA), 10 mg l^{-1} (*2,4*-D), 30 mg l^{-1} (TCE), 100 mg l^{-1} (cBENZ), and 5 mg l^{-1} (atrazine). Specific activity of tritium and ^{14}C-labelled *2,4*-D in the solution was 2.5 and 3.0 nCi ml^{-1}, respectively. Flow rates of 0.35 or 0.03 ml min^{-1} were used for the experiments conducted with the stainless-steel column wherein sorption kinetics were examined. Flow rates of 4.5 or 0.35 ml min^{-1} were used for the larger Plexiglas columns. These yield pore-water velocities of ~ 20 (fast) and ~ 1 (slow) cm h^{-1} for all systems.

3. Data analysis

3.1. Solute transport models

The MPNE model was designed to simulate solute transport in porous media where both transport-related and sorption-related non-ideality are operative. In the MPNE model, the dual-porosity (advective–nonadvective) approach is used to represent physical non-ideality. Sorption is represented by the two-domain approach, with sorption being essentially instantaneous for a portion of the sorbent and rate-limited for the remainder. Sorption may be instantaneous or rate-limited in either of the two porosity domains.

The four dimensionless governing equations for the MPNE model are as follows (Brusseau et al., 1989):

$$R_{a1}\frac{\partial C_a}{\partial T} + k_a^0(C_a^* - S_a^*) + \omega(C_a^* - C_n^*) = \frac{1}{P}\frac{\partial^2 C_a^*}{\partial X^2} - \frac{\partial C_a^*}{\partial X} \tag{1}$$

$$R_{n1}\frac{\partial C_n^*}{\partial T} + k_n^0(C_n^* - S_n^*) = \omega(C_a^* - C_n^*) \tag{2}$$

$$R_{a2}\frac{\partial S_a^*}{\partial T} = k_a^0(C_a^* - S_a^*) \tag{3}$$

$$R_{n2}\frac{\partial S_n^*}{\partial T} = k_n^0(C_n^* - S_n^*) \tag{4}$$

Definitions of the parameters are presented in the Notation. Eqs. (1) and (2) are the mass balances for the advective and non-advective domains, respectively. Eqs. (3) and (4) are balances for the rate-limited sorbed phases in the advective and non-advective domains, respectively.

For the column comprised of the porous spheres and glass beads, physical non-ideality was the only non-ideality factor operative. In this case, the dual porosity conceptualization was used (van Genuchten and Wierenga, 1976). For the column containing the homogeneously packed Mixture soil, rate-limited sorption was the only non-ideality

factor operative. For this case, the two-domain adsorption–desorption approach was used (Selim et al., 1976; Cameron and Klute, 1977).

3.2. Parameter determination

3.2.1. System with rate-limited sorption

The value for the Péclet number is obtained by application of the traditional advective–dispersion equation to nonreactive tracer data (PFBA). The value obtained for the tracer is used for analysis of the sorbing solutes. The retardation factor, R, is calculated by moment analysis. The input pulse, T, is measured from the experiment. The non-ideality parameters are obtained by using a nonlinear least-squares program (FITNLE) that includes nonlinear sorption (Jessup et al., 1989).

3.2.2. System with physical non-ideality

The value for the Péclet number is based on the results of the miscible-displacement experiment for PFBA transport in the column packed with solid glass spheres and glass beads, with the data analyzed with the traditional advection–dispersion equation. This value is used for analysis of the system containing the porous spheres. Values for R are obtained from moment analysis. The input pulse, T, is measured from the experiment. The non-ideality parameters (β, ω) are optimized by using CFITIM3 (van Genuchten, 1981), a nonlinear, least-squares optimization program.

For independent predictions, values of θ_a and θ_n are calculated from the gravimetrically-measured water masses associated with the inter-aggregate and intra-aggregate pore-water domains, respectively. This allows independent calculation of the fraction of the total water content residing in the inter-aggregate region, ϕ.

For the dual-porosity model, the β term [$\beta = (\theta_a + \rho f K_p)/(\theta + \rho K_p)$] represents the fraction of the solute retention that occurs "instantaneously". Note that $\beta = \phi/R$ when f, the mass fraction of sorbent associated with the advective domain (glass beads in this case), is 0. This approach is used considering that solute sorption in this system is associated with the clayey porous spheres and not the glass beads.

Values of ω for the solutes are obtained using values of the first-order mass transfer coefficient (α), which are calculated using the following equation (Rao et al., 1980a) based on mass transfer being predominantly diffusion-controlled:

$$\alpha = \frac{\phi q_1^2}{1-b}\left[\frac{0.1}{T^*}\right]^b, \quad 10^{-4} < T^* \leq 0.1 \tag{5a}$$

and

$$\alpha = \phi q_1^2\left[1 + \frac{0.1b}{(1-b)T^*}\right], \quad T^* \geq 0.1 \tag{5b}$$

where

$$b = 0.14472\ln\left(167/\phi q_1^2\right) \tag{5c}$$

and

$$T^* = \tau D_0 t_r / a^2 \tag{5d}$$

Relevant parameters of the equation are defined in the Notation. Rao et al. (1980a) developed the equation to account for the time dependency of α. The equation provides an averaged α value calculated over the mean column residence time. Time-averaged α values are calculated for each miscible displacement experiment, given the values of ϕ, q_l, τ, D_0, a, and t_r (L/v_a). The values for q_l are taken from Rao et al. (1980a) for the corresponding ϕ values. The tortuosity factor (0.15) is obtained from measured data for $^{36}Cl^-$ and ^3H_2O diffusion in the porous spheres, as reported by Rao et al. (1980a). This value is in good agreement with the values reported by Robin et al. (1987) for diffusion in a compacted mixture of bentonite (50 wt%) and sand. The value of D_0 for ^3H_2O is from Wang et al. (1953), and D_0 for other solutes are estimated by use of the Hayduk and Laudie approach (Tucker and Nelken, 1982).

3.2.3. System with both physical and sorption non-ideality

Given that the advective domain is comprised of the Mixture soil, values of K_a, k_{a2} and F_a for the sorbing solutes are obtained from the column packed with only the Mixture soil. Values of K_n (equilibrium constant for sorption by the clayey porous spheres) are calculated using the results of the breakthrough curves in the column packed with porous spheres and glass beads. Considering the small interactions between the low-polarity organic compounds and the porous spheres made from kaolinite clay suspension, the assumption of instantaneous, linear, and reversible sorption should most likely be valid. With these assumptions, k_{n2} is zero and F_n is 1.

The value of ϕ is calculated from the gravimetrically-measured water masses, as stated above. The mass fraction of sorbent comprising the advective domain, f [e.g., mass ratio of (Mixture soil)/(Mixture soil + porous spheres)], is 0.52 for this system. The f value is one of the most difficult parameters to obtain independently in systems with multiple non-ideality factors. One purpose for using the well-defined systems in this work was to provide a means to calculate the f value.

4. Results and discussion

4.1. Transport in the system with rate-limited sorption

Pertinent properties of the columns and the experimental conditions are presented in Tables 1 and 2. The breakthrough curve for transport of PFBA, a nonreactive tracer, in the Mixture soil column is shown in Fig. 1. A symmetrical breakthrough curve, with minimal early breakthrough and tailing, indicates that there is negligible "immobile" water in the system. The value for the Péclet number ($P = 49.1$) was used for analyzing the transport of the sorbing solutes.

Breakthrough curves for transport of trichloroethene, chlorobenzene, atrazine, and 2,4-D through the Mixture soil are presented in Figs. 1 and 2. The tailing of concentration toward C/C_0 of 1 and 0 is an indication of rate-limited sorption. Two or three parameters (β, ω, and n) were optimized, with values for P, R, and T fixed. The simulated curves matched the data well (Figs. 1 and 2).

Table 1
Properties of the packed columns and selected parameter values

Porous media	Column No.	Column	L (cm)	ρ (g cm^{-3})	T_0 (cm^3)	θ (cm^3 cm^{-3})	θ_a (cm^3 cm^{-3})	θ_n (cm^3 cm^{-3}	ϕ	a
Homogeneous medium:										
Mixture soil	stainless steel	A	7.0	1.65	9.07	0.37	0.37	–	1.0	–
Nonreactive [a] *aggregated medium*:										
Porous spheres in glass beads	Plexiglas	B	15.0	1.65	263.4	0.39	0.25	0.14	0.64	0.55
Reactive aggregated medium:										
Porous spheres in mixture soil	Plexiglas	C	15.0	1.48	301.3	0.44	0.30	0.14	0.68	0.55

[a] Nonreactive or slightly reactive.

Sorption appeared to be slightly nonlinear (Freundlich exponent $n \approx 0.86$) for *2,4*-D in the Mixture soil under both fast and slow pore-water velocities. Another optimization was done by fixing $n = 1$. Comparison of the optimized simulations (Fig. 2) shows an insignificant effect of not considering nonlinear sorption. Hence, sorption-kinetics parameters based on linear sorption (listed in Table 3) will be used as inputs for the MPNE model predictions.

There is a difference in sorption kinetics parameters for both *2,4*-D and atrazine between fast and slow pore-water velocities. While values of β and ω changed only slightly, the desorption rate coefficient k_2 decreased approximately an order of magnitude with an order-of-magnitude decrease in pore-water velocity. The dependency of k_2 on pore-water velocity has been reported previously (Gamerdinger et al., 1991; Brusseau, 1992; Kookana et al., 1993; Gaber et al., 1995). The dependency noted in this study is further indication of a physical process such as diffusion into/out of components of the solid phase being the limiting factor for sorption kinetics, as the time available for diffusion is inversely related to pore-water velocity. The value for F, the fraction of sorbent for which sorption is instantaneous, is larger for the slow pore-water velocity.

4.2. Transport in the system with physical non-ideality

The breakthrough curves obtained for transport of ^3H_2O, PFBA, *2,4*-D, and atrazine through the column packed with the porous spheres and glass beads are presented in Figs. 3 and 4. The asymmetrical and tailed breakthrough curve for PFBA, a nonreactive and non-sorbing solute (retardation factor close to 1), indicates the effect of the structured porous medium on solute transport.

An optimized value of 90 for the Péclet number was obtained for the column packed with the solid spheres and glass beads. Values for K_n, calculated from R, represent solute interaction with the porous spheres. The retardation factor for ^3H_2O was ~ 1.2, suggesting a slight interaction in the system. Other studies have also revealed slight

Table 2
Conditions of the experimental systems and selected parameter values

Medium	Column No.	Exp. No.	Solute	q (cm h^{-1})	v (cm h^{-1})	v_a (cm h^{-1})	T	R
Homogeneous	A	A-1	PFBA	11.5	31.5	31.5	9.17	0.99
	A	A-2	2,4-D	6.46	17.6	17.6	18.49	3.42
	A	A-3	TCE	6.53	17.8	17.8	25.21	4.78
	A	A-4	cBENZ	6.05	16.5	16.5	9.13	7.27
	A	A-5	atrazine	6.41	17.5	17.5	13.23	9.10
	A	A-6	2,4-D	0.51	1.40	1.40	14.36	3.79
	A	A-7	atrazine	0.52	1.42	1.42	10.20	10.8
	A	A-8	^{14}C 2,4-D	5.91	16.1	16.1	19.12	– [a]
	A	A-9	^{14}C 2,4-D	5.87	16.0	16.0	21.68	– [a]
Nonreactive aggregated	B	B-1	$^{3}H_2O$	5.73	14.8	23.3	3.37	1.20
	B	B-2	PFBA	6.12	15.8	24.9	4.57	1.04
	B	B-3	PFBA	4.69	12.1	19.0	2.88	1.03
	B	B-4	2,4-D	6.04	15.6	24.6	3.65	1.16
	B	B-5	TCE	5.96	15.4	24.2	3.62	1.14
	B	B-6	atrazine	5.13	13.3	20.9	3.10	1.18
Reactive aggregated	C	C-1	$^{3}H_2O$	5.81	13.1	19.4	4.87	1.17
	C	C-2	PFBA	5.81	13.1	19.4	4.87	1.07
	C	C-3	PFBA	6.74	15.2	22.5	5.50	1.06
	C	C-4	2,4-D	5.37	12.1	17.9	5.34	1.93
	C	C-5	TCE	7.33	16.5	24.4	9.42	2.73
	C	C-6	cBENZ	5.22	11.8	17.4	5.79	3.38
	C	C-7	atrazine	6.14	13.8	20.5	9.15	4.01
	C	C-8	$^{3}H_2O$	0.46	1.03	1.53	3.35	1.17
	C	C-9	PFBA	0.46	1.03	1.53	3.35	1.08
	C	C-10	2,4-D	0.43	0.98	1.44	3.48	2.11
	C	C-11	atrazine	0.46	1.04	1.53	2.78	4.57
	C	C-12	^{14}C 2,4-D	5.78	18.1	12.2	5.72	– [a]
	C	C-13	^{14}C 2,4-D	5.83	18.2	12.4	5.77	– [a]

[a] experiments with flow interruption.

retardation of $^{3}H_2O$ in soil column studies (Wierenga et al., 1975; van Genuchten and Wierenga, 1977; Seyfried and Rao, 1989; Gaber et al., 1995). The interaction has been postulated to occur via hydroxyl exchange on clay lattices.

The optimized simulations produced with the first-order, dual-porosity model reproduce the data well. This confirms the work of Hu and Brusseau (1995) that this model can be used to approximate solute transport in the aggregated medium evaluated herein. An attempt was also made to predict the breakthrough curves by using independently determined parameter values. The predictions derived from the independently determined values for P, R, β, and ω matched the experimental data quite well (see Figs. 3 and 4). Similarly, the predicted values for β and ω are quite comparable to optimized values (Table 4). This illustrates the applicability of using Eqs. 5 for calculating α values for this system.

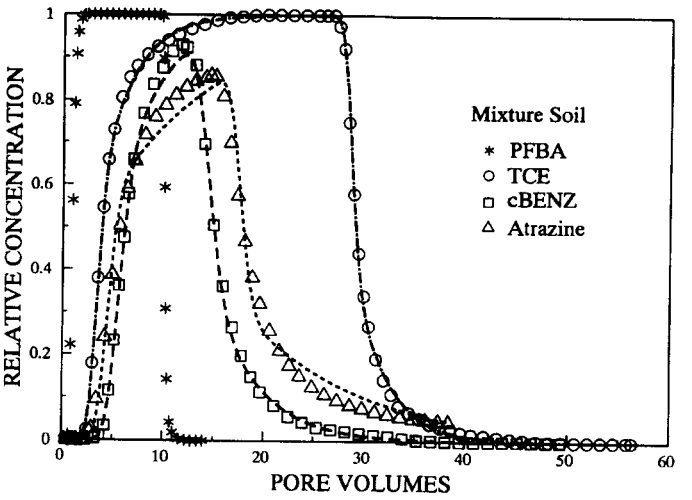

Fig. 1. Breakthrough curves for transport of PFBA, trichloroethene, chlorobenzene, and atrazine through the homogeneous Mixture soil column (*points* = experimental data; *lines* = simulations produced with the two-domain sorption model).

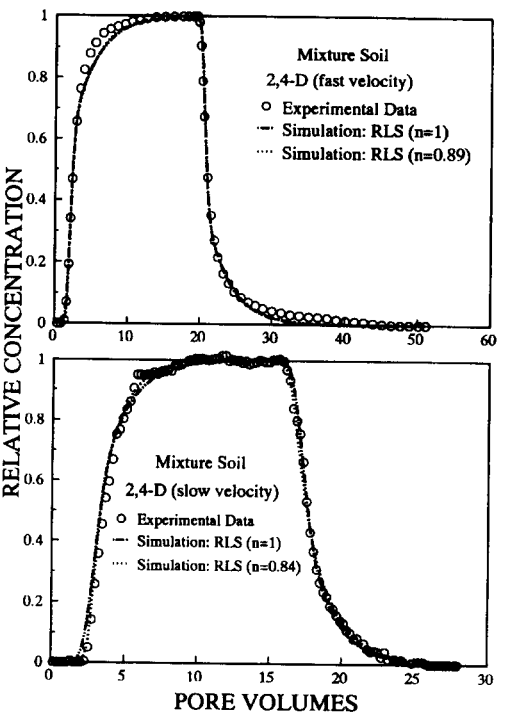

Fig. 2. Breakthrough curves (*data points*) and simulations produced with the two-domain sorption model (*line*) for transport of 2,4-D in Mixture soil: (A) fast pore-water velocity; and (B) slow pore-water velocity (*RLS* = rate-limited sorption only).

Table 3
Sorption kinetics parameters for Mixture soil [a]

Solute	Exp. No.	β [b]	ω [b]	K_a (ml g^{-1})	k_{a2} (h^{-1})	F_a
2,4-D	A-2	0.64 (0.63–0.65)	0.48 (0.44–0.51)	0.54	0.98 (0.88–1.07)	0.49 (0.48–0.50)
TCE	A-3	0.73 (0.72–0.73)	0.52 (0.50–0.54)	0.84	1.02 (0.96–1.08)	0.66 (0.65–0.66)
cBENZ	A-4	0.78 (0.77–0.78)	0.45 (0.42–0.48)	1.39	0.66 (0.60–0.73)	0.74 (0.74–0.75)
Atrazine	A-5	0.50 (0.49–0.51)	0.56 (0.53–0.60)	1.80	0.31 (0.28–0.33)	0.44 (0.43–0.45)
2,4-D	A–6	0.77 (0.76–0.78)	0.62 (0.54–0.69)	0.62	0.14 (0.12–0.17)	0.69 (0.68–0.71)
Atrazine	A-7	0.59 (0.59–0.60)	0.71 (0.69–0.73)	2.19	0.033 (0.031–0.034)	0.55 (0.55–0.56)

[a] Values in parentheses represent 95% confidence intervals.
[b] β and ω presented here are optimized with Freundlich exponent fixed at 1 ($n = 1$).

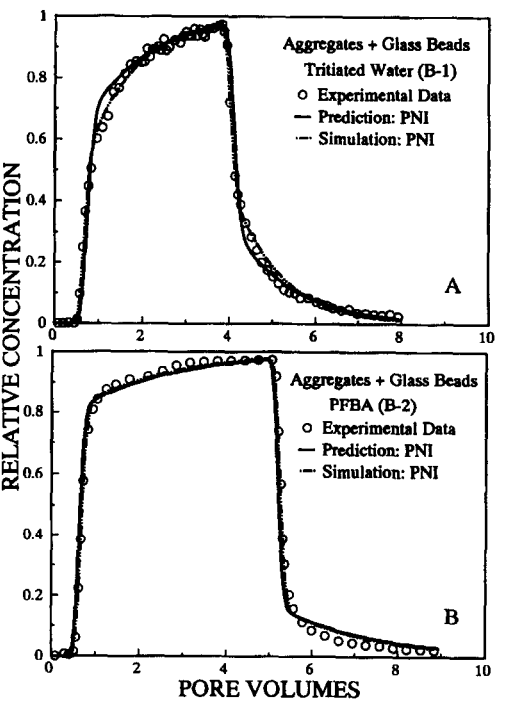

Fig. 3. Experimental data, predicted and optimized simulations produced with the dual-porosity model for transport of non-reactive tracers in the column packed with the porous spheres and glass beads: (A) ^3H_2O; and (B) PFBA (*PNI* = physical non-ideality only).

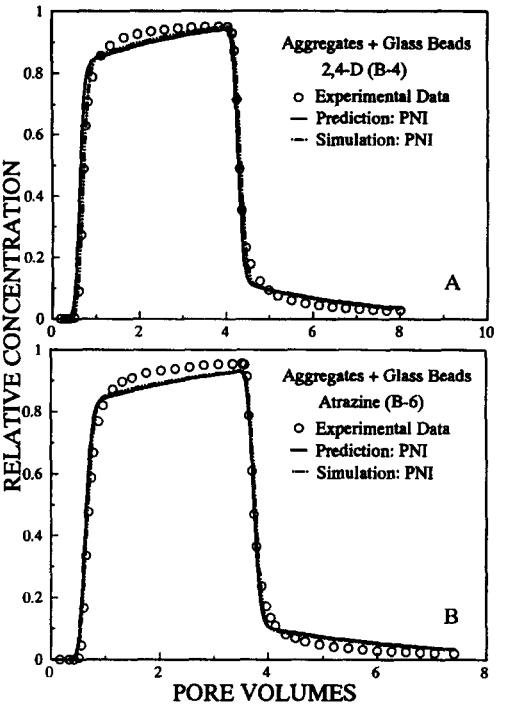

Fig. 4. Experimental data, prediction and optimized simulations produced with the dual-porosity model for transport of reactive-solute in the column packed with the porous spheres and glass beads: (A) *2,4*-D; and (B) atrazine.

Table 4
Predicted and optimized parameter values for physical non-ideality [a]

Exp. No.	Solute	β		ω		α (h^{-1})	
		predicted	optimized	predicted	optimized	predicted	optimized
B-1	^3H_2O	0.53	0.58 (0.57--0.59)	0.40	0.63 (0.59--0.67)	0.15	0.24 (0.22–0.26)
B-2	PFBA	0.61	0.66 (0.65--0.66)	0.20	0.19 (0.17--0.21)	0.083	0.078 (0.069–0.086)
B-3	PFBA	0.62	0.63 (0.63--0.64)	0.24	0.20 (0.18--0.22)	0.074	0.062 (0.056–0.069)
B-4	*2,4*-D	0.55	0.62 (0.61--0.62)	0.19	0.18 (0.15--0.20)	0.076	0.072 (0.062–0.082)
B-5	TCE	0.56	0.59 (0.59--0.60)	0.23	0.22 (0.20--0.24)	0.092	0.087 (0.079–0.095)
B-6	atrazine	0.54	0.57 (0.56--0.58)	0.19	0.18 (0.14--0.21)	0.065	0.062 (0.048–0.072)
C-1	^3H_2O	0.58	0.58 (0.56--0.59)	0.38	0.53 (0.47--0.59)	0.14	0.20 (0.18–0.23)
C-2	PFBA	0.63	0.57 (0.56--0.58)	0.20	0.33 (0.30--0.36)	0.077	0.13 (0.12–0.14)
C-8	^3H_2O	0.58	0.55 (0.53--0.58)	1.97	1.40 (1.24--1.54)	0.060	0.043 (0.038–0.047)
C-9	PFBA	0.63	0.63 (0.62--0.65)	0.84	0.60 (0.54--0.66)	0.026	0.018 (0.017–0.020)

[a] Values in parentheses represent 95% confidence intervals.

4.3. Transport in the system with both physical and sorption non-ideality

4.3.1. MPNE *model prediction*

The asymmetrical and tailed breakthrough curve for transport of PFBA and ^3H_2O in the column packed with porous spheres and Mixture soil indicates the effect of soil structure on solute transport. It is expected that this effect will also influence the transport of sorbing solutes in the system. For transport of PFBA and ^3H_2O, the dual-porosity model was appropriate and predicted the breakthrough curves quite well (^3H_2O data shown in Fig. 5a as an example), similar to the column packed with porous spheres and glass beads.

The breakthrough curves for the reactive solutes also exhibit non-ideality (see Figs. 6 and 7), which in this case is caused by some combination of rate-limited sorption and physical non-ideality. As such, predictions accounting for physical non-ideality or rate-limited sorption alone would not fully reproduce the experimental data for the sorbing solutes, as exemplified by the *2,4*-D and atrazine data (Fig. 6). The non-ideal transport of these sorbing solutes in the structured medium is caused by contributions from both physical non-ideality and rate-limited sorption. The MPNE model, with the incorporation of both non-ideality factors, may be suitable in this case.

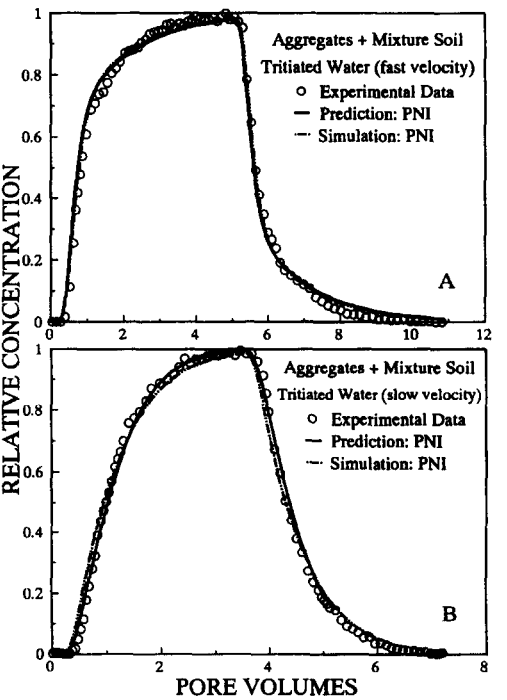

Fig. 5. Experimental data, prediction and optimized simulations produced with the dual-porosity model for transport of ^3H_2O in the column packed with the porous spheres and Mixture soil at: (A) fast pore-water velocity; and (B) slow pore-water velocity.

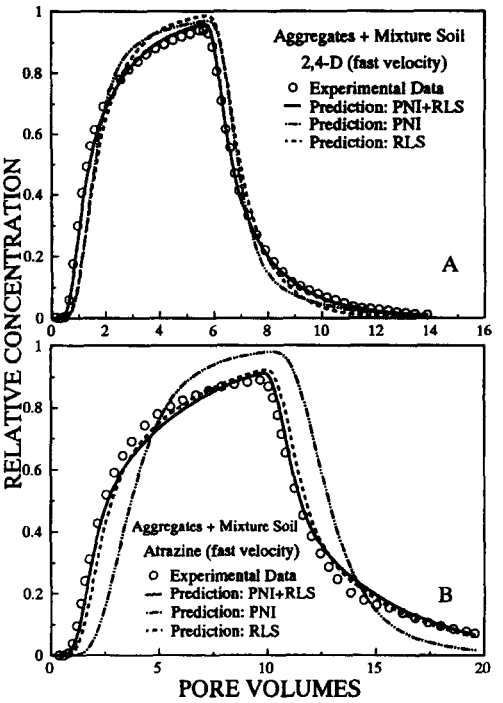

Fig. 6. Experimental data and predictions produced with three different models for transport in the column packed with the porous spheres and Mixture soil: (A) *2,4*-D; and (B) atrazine. (*RLS* + *PNI* = considering both rate-limited sorption and physical non-ideality, e.g., MPNE model)

Independently determined parameters for MPNE model predictions are presented in Table 5. The Péclet number (13.8) for the column was obtained from the fit of the dual-porosity model to the breakthrough curve of PFBA (exp. No. C-3), with R and T fixed. This Péclet number was used for all other data sets obtained with this column. Values of α were calculated with Eqs. 5, and discussion in the previous section has shown this approach is adequate for the system examined herein.

Values of K_a, k_{a2} and F_a for the Mixture soil (the advective domain) are listed in Table 3. Values of K_n for the sorbing solutes, except for chlorobenzene, were calculated using the results from the column packed with porous spheres and glass beads; K_n for chlorobenzene is assumed to be 0.036 ml g^{-1}, similar to that for *2,4*-D, TCE, and atrazine. As discussed previously, k_{n2} is set equal to zero and F_n is 1. The independently determined global equilibrium sorption constants $[fK_a + (1-f)K_n]$ and global retardation factors are listed in Table 5. The predicted R values are in good agreement with the values obtained from moment analysis of the breakthrough curves (presented in Table 2). With the above inputs, the non-dimensional parameters (β_1, β_2, β_3, β_4, k_a^0, k_n^0) required for the MPNE model can be calculated.

Independent predictions for transport of the sorbing solutes, obtained with the MPNE model, are shown in Figs. 6 and 7. Inspection reveals that the predictions match the experimental data quite well. This is encouraging considering that all input parameters

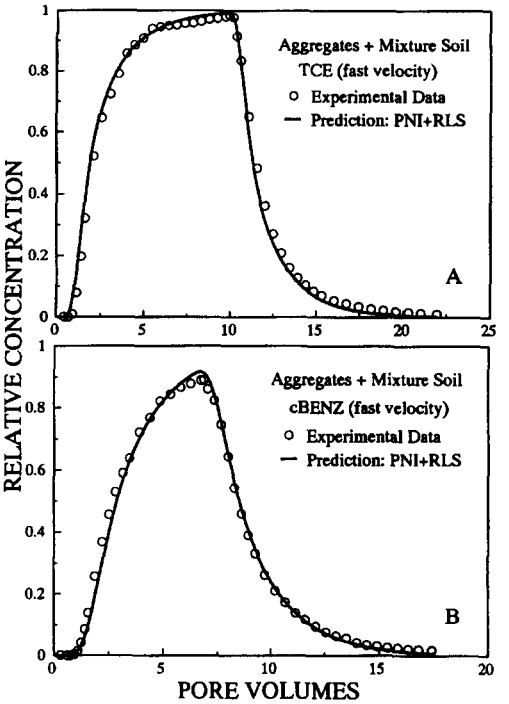

Fig. 7. Experimental data and predictions produced with the MPNE model for transport in the column packed with the porous spheres and Mixture soil: (A) TCE; and (B) chlorobenzene.

Table 5
Independently determined parameters for MPNE model prediction in Mixture soil with the porous spheres [a]

Exp. No.	^3H_2O C-1	PFBA C-2	2,4-D C-4	TCE C-5	cBENZ C-6	Atrazine C-7	^3H_2O C-8	PFBA C-9	2,4-D C-10	Atrazine C-11
D_0 (cm^2 h^{-1})	0.088	0.028	0.024	0.035	0.033	0.021	0.088	0.028	0.024	0.021
α (h^{-1})	0.15	0.078	0.069	0.097	0.081	0.067	0.062	0.027	0.023	0.022
ω	0.38	0.20	0.19	0.20	0.23	0.16	1.97	0.84	0.79	0.70
K_n (ml g^{-1})	0.043	0	0.035	0.030	0.036	0.038	0.043	0	0.035	0.038
F_n	1	1	1	1	1	1	1	1	1	1
k_{n2} (h^{-1})	0	0	0	0	0	0	0	0	0	0
K_p (ml g^{-1})	0.021	0	0.29	0.45	0.74	0.95	0.021	0	0.34	1.15
R	1.07	1.0	1.98	2.50	3.47	4.17	1.07	1.0	2.13	4.84
β_1	0.63	0.68	0.57	0.65	0.71	0.49	0.63	0.68	0.67	0.57
β_2	0	0	0.24	0.20	0.18	0.42	0	0	0.15	0.35
β_3	0.37	0.32	0.19	0.15	0.11	0.092	0.37	0.32	0.18	0.079
β_4	0	0	0	0	0	0	0	0	0	0
k_a^0	0	0	0.57	0.46	0.52	0.58	0	0	0.72	0.80
k_n^0	0	0	0	0	0	0	0	0	0	0

[a] Values for K_a, k_{a2} and F_a are listed in Table 3.

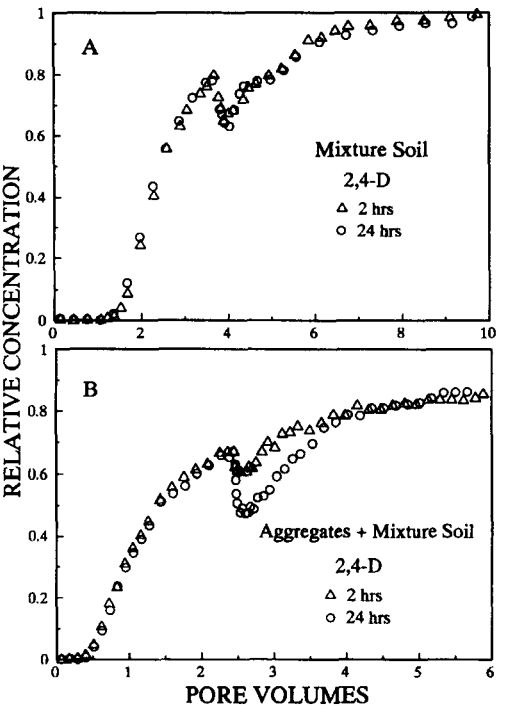

Fig. 8. Effect of duration in flow interruption on *2,4*-D transport: (A) Mixture soil column; and (B) column packed with the porous spheres and Mixture soil.

for the predictions are obtained independently. It also demonstrates that the MPNE model adequately represents the processes controlling the transport of rate-limited sorbing solutes in the aggregated system. Furthermore, it appears that the first-order bicontinuum approach can be used to represent diffusive mass transfer processes for both rate-limited sorption and physical non-ideality in the system.

4.3.2. Synergetic effects of non-ideality

The β terms represent the amount of retardation associated with each of the four sorptive domains. For this system, $> 80\%$ (i.e. $\beta_1 + \beta_2$) of retardation is associated with the Mixture soil, which is expected. The relative importance of the factors contributing to non-ideality can also be evaluated by comparing the magnitudes of the respective Damköhler numbers (Brusseau et al., 1989). Based on Fig. 6, it appears that physical non-ideality and rate-limited sorption provide similar contributions to non-ideal transport for *2,4*-D, while rate-limited sorption comprises the major contribution to non-ideality of atrazine transport. The figures show that the synergistic effect of multiple non-ideality factors will impact solute transport.

Flow interruption provided additional evidence with regard to the synergistic effect of the two non-ideality factors. Two durations of interruption (namely, 2 and 24 h) were performed during transport of ^{14}C-labeled *2,4*-D in two soil systems under similar

pore-water velocities. Inspection of Fig. 8 reveals that there is little difference between the results of the two experiments for *2,4*-D in the Mixture soil column, which indicates that sorption has reached equilibrium within 2 h. Conversely, in the system with both sorption and physical non-ideality, an interruption duration of 24 h showed a larger concentration change than that for 2 h. The additional concentration change is associated with rate-limited mass transfer between inter-aggregate and intra-aggregate pore-water domains. These results are supported by data reported for PFBA, which has an aqueous diffusion coefficient similar to that of *2,4*-D. The magnitudes of the concentration change increased with increasing interruption time of 2, 4, and 8 h in a column packed with porous spheres and glass beads (Hu and Brusseau, 1995).

To summarize, we observed, on one hand, that physical non-ideality has a larger characteristic "reaction" time compared to rate-limited sorption, and, therefore, could be controlling transport. However, analysis of mass distribution shows that the majority of retention is associated with sorption, suggesting sorption would be controlling. The fact that both are of roughly equal importance for *2,4*-D transport illustrates that both mass distribution and characteristic reaction time are important factors influencing transport. With use of the MPNE model, it was possible to quantify the relative contributions of these factors.

4.3.3. Dependency of α and k_2 with pore-water velocity

Since diffusive mass transfer is a rate-limited process, residence time is expected to affect the magnitude of observed non-ideality. Breakthrough curves for transport of ^3H_2O at fast ($v_a = 19.4$ cm h^{-1}, exp. No. C-1) and slow ($v_a = 1.53$ cm h^{-1}, exp. No. C-8) pore-water velocities through the column packed with the porous spheres and Mixture soil are shown in Fig. 5. A smaller degree of non-ideal transport is observed for the slow velocity. Optimized simulations based on the dual-porosity model reproduce both sets of data (Fig. 5b). The same is true for PFBA (data not shown). The optimized values of α decrease with a decrease in the pore-water velocity (Table 4). This behavior has been observed and discussed by others (van Genuchten and Wierenga, 1977; Rao et al., 1980b; Nkedi-Kizza et al., 1983; Herr et al., 1989; Brusseau, 1991).

A theoretical relationship showing the mass-transfer coefficient to be a function of time was presented by Rao et al. (1980a). Because the time available for diffusion into and out of the non-advective pore-water domains is inversely related to pore-water velocity, α is expected to decrease with decreasing pore-water velocity. An additional factor is the possibility of advective mixing occurring inside the "immobile" domains. Such a mixing process would effectively increase the value of α, given that the mobile-immobile model is based on an assumption that solute exchange between mobile and immobile domains occurs only by diffusion. The relative contribution of advective mixing may vary with velocity, thus contributing to an observed velocity dependency of α. Furthermore, it is well known that the definition of "immobile" water is system- and condition-dependent. This also can play a part in the velocity dependency of α.

Eqs. 5, proposed by Rao et al. (1980a), incorporate the velocity effect (i.e. the mean column residence time) in calculating α values. The predicted α values for ^3H_2O and PFBA are quite close to the optimized α values for both the fast (exp. Nos. C-1, -2) and slow (exp. Nos. C-8, -9) pore-water velocities (Table 4). As noted before, the mean

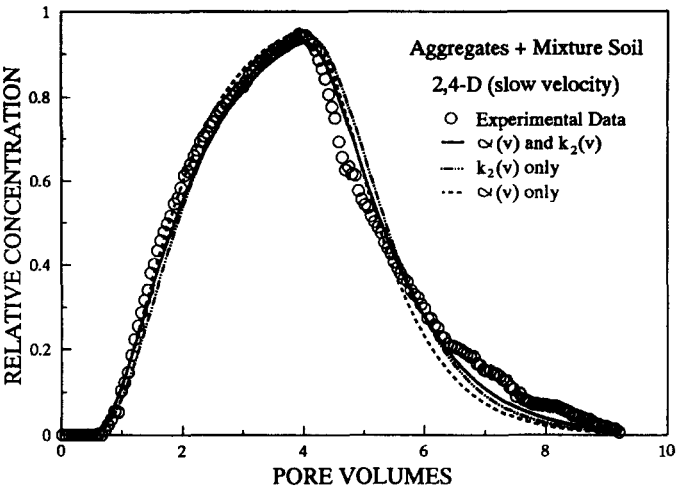

Fig. 9. Experimental data and MPNE model prediction for transport of *2,4*-D under slow pore-water velocity in the column packed with the porous spheres and Mixture soil.

column residence time is chosen as the time period over which the average α is calculated. It appears that accounting for the residence-time effect is sufficient to explain the velocity dependency of α for the system herein.

Figs. 9 and 10 show predictions for transport of *2,4*-D and atrazine at the slow pore-water velocity under three scenarios. The values of α for *2,4*-D and atrazine (in Table 5) are calculated by Eqs. 5. The best match is obtained by considering both α and k_2 as functions of pore-water velocity. Note that the contributions of rate-limited

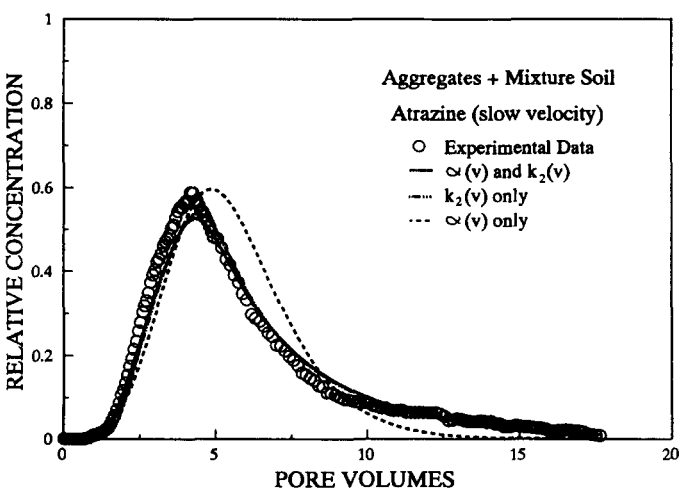

Fig. 10. Experimental data and MPNE model prediction for transport of atrazine under slow pore-water velocity in the column packed with the porous spheres and Mixture soil.

sorption and physical non-ideality to non-ideal transport for *2,4*-D and atrazine are consistent with that discussed for the fast pore-water velocity. For atrazine, the prediction based on ignoring the velocity-dependency of k_2 (using k_2 value derived from the fast-velocity experiment) will cause significant deviation from the experimental data. The implication of decreasing α and k_2 with decreasing velocity for solute transport should be accounted for in process-specific investigations.

5. Conclusions

In field situations, transport of reactive solutes can be influenced by both physical non-ideality and rate-limited sorption, among other factors. The impact of multiple non-ideality factors on contaminant transport and remediation needs to be assessed. This work was a step in this direction by investigating contaminant transport in well-defined systems. The synergistic effects of multiple non-ideality factors were examined for their impact on solute transport. Flow interruption has been shown to provide additional evidence with regard to the synergistic effects of multiple non-ideality factors. Our analyses have shown that both mass distribution and characteristic reaction time are important factors influencing transport.

6. Notation

a = sphere radius [L]
C_0 = input solute concentration [M L^{-3}]
C_a = solute concentration in the advective domain [M L^{-3}]
C_n = solute concentration in the non-advective domain [M L^{-3}]
C_a^* = C_a/C_0, dimensionless solute concentration
C_n^* = C_n/C_0, dimensionless solute concentration
D = hydrodynamic dispersion coefficient [L^2 T^{-1}]
D_0 = aqueous diffusion coefficient of the solute [L^2 T^{-1}]
f = mass fraction of sorbent comprising the advective domain (dimensionless)
F_a = fraction of sorbent in the advective domain for which sorption is instantaneous (dimensionless)
F_n = fraction of sorbent in the non-advective domain for which sorption is instantaneous (dimensionless)
k_{a2} = first-order desorption rate coefficient in the advective domain [T^{-1}]
k_{n2} = first-order desorption rate coefficient in the non-advective domain [T^{-1}]
k_a^0 = $k_{a2}L\theta R_{a2}/q$, Damköhler number representing contribution of sorption non-ideality in the advective domain (dimensionless)
k_n^0 = $k_{n2}L\theta R_{n2}/q$, Damköhler number representing contribution of sorption non-ideality in the non-advective domain (dimensionless)

K_a = equilibrium sorption constant for the advective domain [L^3 M^{-1}]
K_n = equilibrium sorption constant for the non-advective domain [L^3 M^{-1}]
K_p = global equilibrium sorption constant [L^3 M^{-1}]
L = length of interest [L]
n = Freundlich intensity parameter (dimensionless)
P = $qL/\theta_a D$, Péclet number (dimensionless)
q = Darcy flux [L T^{-1}]
q_1 = empirical constant related to the ϕ value (dimensionless)
R = $R_{a1} + R_{a2} + R_{n1} + R_{n2} = 1 + (\rho/\theta)K_p$, the global retardation factor (dimensionless)
R_{a1} = $[\phi + f(\rho/\theta)F_a K_a]/R$, retardation in the instantaneous sorbed phase of the advective domain (dimensionless)
R_{a2} = $[f(\rho/\theta)(1 - F_a)K_a]/R$, retardation in the rate-limited sorbed-phase of the advective domain (dimensionless)
R_{n1} = $[(1 - \phi) + (1 - f)(\rho/\theta)F_n K_n]/R$, retardation in the instantaneous sorbed − phase of the non-advective domain (dimensionless)
R_{n2} = $[(1 - f)(\rho/\theta)(1 - F_n)K_n]/R$, retardation in the rate-limited sorbed phase of the non-advective domain (dimensionless)
S_{a2} = mass of sorbate in rate-limited sorbed phase divided by the mass of sorbent in the advective domain [M M^{-1}]
S_{n2} = mass of sorbate in rate-limited sorbed phase divided by mass of sorbent in the non-advective domain [M M^{-1}]
S_a^* = $S_{a2}/[(1 - F_a)K_a C_0]$ (dimensionless)
S_n^* = $S_{n2}/[(1 - F_n)K_n C_0]$ (dimensionless)
t_r = mean column residence time [T^{-1}]
T = $qt/\theta L$, dimensionless time in pore volumes
T_0 = column pore volume [L^3]
T^* = $\tau D_0 t_r/a^2$, dimensionless time
v_a = q/θ_a, average pore water velocity in the advective domain [L T^{-1}]
X = x/L, dimensionless length
α = first-order mass transfer coefficient [T^{-1}]
β_1 = R_{a1}/R, fractional retardation parameter (dimensionless)
β_2 = R_{a2}/R, fractional retardation parameter (dimensionless)
β_3 = R_{n1}/R, fractional retardation parameter (dimensionless)
β_4 = R_{n2}/R, fractional retardation parameter (dimensionless)
β = fraction of instantaneous retardation (dimensionless)
θ = $\theta_a + \theta_n$, total volumetric water content [L^3 L^{-3}]
θ_a = volumetric water content in the advective domain [L^3 L^{-3}]
θ_n = volumetric water content in the non-advective domain [L^3 L^{-3}]
ρ = bulk density [M L^{-3}]
τ = tortuosity factor for the non-advective domain (dimensionless)
ϕ = θ_a/θ (dimensionless)
ω = $\alpha L/q$, the Damköhler number (a ratio of hydrodynamic residence time to characteristic reaction time) representing contribution of the physical non-ideality (dimensionless)

Acknowledgements

This research was supported by a project funded under the U.S. Department of Agriculture National Research Initiative Competitive Grants Program (Water Resources Assessment and Protection Division). We thank Dr. P.S.C. Rao, University of Florida, who kindly lent us the porous ceramic spheres.

References

Brusseau, M.L., 1991. Application of a multiprocess non-equilibrium sorption model to solute transport in a stratified porous medium. Water Resour. Res., 27(4): 589–595.

Brusseau, M.L., 1992. Nonequilibrium transport of organic chemicals: The impact of pore-water velocity. J. Contam. Hydrol., 9: 353–368.

Brusseau, M.L., 1994. Transport of reactive contaminants in heterogeneous porous media. Rev. Geophys., 32: 285–313.

Brusseau, M.L. and Zachara, J.M., 1993. Transport of Co^{2+} in a physically and chemically heterogeneous porous medium. Environ. Sci. Technol., 27(9): 1937–1939.

Brusseau, M.L., Jessup, R.E. and Rao, P.S.C., 1989. Modeling the transport of solutes influenced by multi-process non-equilibrium. Water Resour. Res., 25(9): 1971–1988.

Cameron, D.R. and Klute, A., 1977. Convective–dispersive solute transport with a combined equilibrium and kinetic adsorption model. Water Resour. Res., 13(1): 183–188.

Davidson, J.M. and McDougal, J.R., 1973. Experimental and predicted movement of three herbicides in a water-saturated soil. J. Environ. Qual., 2(4): 428–433.

Estrella, M.R., Brusseau, M.L., Maier, R.S., Pepper, I.L., Wierenga, P.J. and Miller, R.M., 1993. Biodegradation, sorption, and transport of *2,4*-dichlorophenoxyacetic acid in saturated and unsaturated soils. Appl. Environ. Microbiol., 59: 4266–4273.

Gaber, H.M., Inskeep, W.P., Comfort, S.D. and Wraith, J.M., 1995. Non-equilibrium transport of atrazine through large intact soil cores. Soil Sci. Soc. Am. J., 59: 60–67.

Gamerdinger, A.P., Lemley, A.T. and Wagenet, R.J., 1991. Nonequilibrium sorption and degradation of three 2-chloro-*s*-triazine herbicides in soil–water systems. J. Environ. Qual., 20: 815–822.

Green, R.E., Yamane, V.K. and Obien, S.R., 1968. Transport of atrazine in a latosolic soil in relation to adsorption, degradation, and soil water variables. 9th Int. Congr. Soil Sci. Trans., Adelaide, S.A., I: 195–204.

Herr, M., Schafer, G. and Spitz, K., 1989. Experimental studies of mass transport in porous media with local heterogeneities. J. Contam. Hydrol., 4(2): 127–137.

Hu, Q. and Brusseau, M.L., 1995. The effect of solute size on transport in structured porous media. Water Resour. Res., 31(7): 1637–1646.

Jessup, R.E., Brusseau, M.L. and Rao, P.S.C., 1989. Modeling solute transport. Fla. Agric. Exp. Stn. Rep., Univ. of Florida.

Kay, B.D. and Elrick, D.E., 1967. Adsorption and movement of lindane in soils. Soil Sci., 104(5): 314–322.

Kookana, R.S., Schuller, R.D. and Aylmore, L.A.G., 1993. Simulation of simazine transport through soil columns using time-dependent sorption data measured under flow conditions. J. Contam. Hydrol., 14(2): 93–115.

Nkedi-Kizza, P., Biggar, J.W., van Genuchten, M.Th., Wierenga, P.J., Selim, H.M., Davidson, J.M. and Nielsen, D.R., 1983. Modeling tritium and chloride 36 transport through an aggregated Oxisol. Water Resour. Res., 19(3): 691–700.

O'Dell, J.D., Wolt, J.D. and Jardine, P.M., 1992. Transport of imazethapyr in undisturbed soil columns. Soil Sci. Soc. Am. J., 56(6): 1711–1715.

Rao, P.S.C., Green, R.E., Balasubramanian, V. and Kanehiro, Y., 1974. Field study of solute movement in a highly aggregated Oxisol with intermittent flooding, II. Picloram. J. Environ. Qual., 3(3): 197–202.

Rao, P.S.C., Rolston, D.E., Jessup, R.E. and Davidson, J.M., 1980a. Solute transport in aggregated porous media: Theoretical and experimental evaluation. Soil Sci. Soc. Am. J., 44(6): 684–688.

Rao, P.S.C., Jessup, D.E., Rolston, R.E., Davidson, J.M. and Kilcrease, D.P., 1980b. Experimental and mathematical description of non-adsorbed solute transfer by diffusion in spherical aggregates. Soil Sci. Soc. Am. J., 44(6): 684–688.

Robin, M.J.L., Gillham, R.W. and Oscarson, D.W., 1987. Diffusion of strontium and chloride in compacted clay-based materials. Soil Sci. Soc. Am. J., 40: 651–655.

Selim, H.M., Davidson, J.M. and Mansell, R.S., 1976. Evaluation of a two-site adsorption–desorption model for describing solute transport in soil. Paper presented at Proc. Summer Computer Simulation Conf., Natl. Sci. Found., Washington, DC, July 12–14, 1976.

Seyfried, M.S. and Rao, P.S.C., 1989. Solute transport in undisturbed columns of an aggregated tropical soil: Preferential flow effects. Soil Sci. Soc. Am. J., 51: 1434– 1444.

Tucker, W.A. and Nelken, L.H., 1982. Diffusion coefficients in air and water. In: W.J. Lyman, W.F. Reehl and D.H. Rosenblatt (Editors), Handbook of Chemical Property Estimation Methods: Environmental Behavior of Organic Compounds. McGraw-Hill, New York, NY, pp. 17-1–17-25.

van Genuchten, M.Th., 1981. Nonequilibrium transport parameters from miscible displacement experiments. U.S. Dep. Agric., Salin. Lab., Riverside, CA, Res. Rep. 119, .

van Genuchten, M.Th. and Wierenga, P.J., 1976. Mass transfer studies in sorbing porous media, 1. Analytical solutions. Soil Sci. Soc. Am. J., 40(4): 473–480.

van Genuchten, M.Th. and Wierenga, P.J., 1977. Mass transfer studies in sorbing porous media, 2. Experimental evaluation with tritium (^3H_2O). Soil Sci. Soc. Am. J., 41(2): 272–278.

van Genuchten, M.Th., Wierenga, P.J. and O'Connor, G.A., 1977. Mass transfer studies in sorbing porous media: 3. Experimental evaluation with 2,4,5-T. Soil Sci. Soc. Am. J., 41(2): 278–285.

Veeh, R.H., Inskeep, W.P., Roe, F.L. and Ferguson, A.H., 1994. Transport of chlorsulfuron through soil columns. J. Environ. Qual., 23: 542–549.

Wang, J.H., Robinson, C.V. and Edelman, I.S., 1953. Self-diffusion and structure of liquid water, III. Measurement of the self-diffusion of liquid water with H^2, H^3, and O^{18} as tracers. J. Am. Chem. Soc., 75: 466–470.

Wierenga, P.J., van Genuchten, M.Th. and Boyle, F.W., 1975. Transfer of boron and tritiated water through sandstone. J. Environ. Qual., 4(1): 83–87.

Zurmuhl, T., Durner, W. and Herrmann, R., 1991. Transport of phthalate-esters in undisturbed and unsaturated soil columns. J. Contam. Hydrol., 8: 111–133.